PERGAMON

Journal of Structural Geology 26 (2004) 29–46

JOURNAL OF STRUCTURAL GEOLOGY

www.elsevier.com/locate/jsg

An AMS, structural and paleomagnetic study of quaternary deformation in eastern Sicily

Francesca Cifelli[a,*], Federico Rossetti[a], Massimo Mattei[a], Ann Marie Hirt[b], Renato Funiciello[a], Luigi Tortorici[c]

[a]*Dipartimento di Scienze Geologiche Università "Roma Tre", Largo S.L. Murialdo 1, 00146 Rome, Italy*
[b]*Insitut für Geophysik, ETH-Hönggerberg, 8093 Zurich, Switzerland*
[c]*Istituto di Geologia e Geofisica, Università di Catania, Corso Italia 55, 95129 Catania, Italy*

Received 17 September 2002; received in revised form 12 May 2003; accepted 15 May 2003

Abstract

An integrated structural, anisotropy of magnetic susceptibility (AMS) and paleomagnetic study was carried out on Plio-Pleistocene sedimentary basins in eastern Sicily. These basins belong to three main tectonic domains: the Tyrrhenian hinterland domain, the Catania foredeep domain, and the Hyblean foreland domain. We sampled 329 oriented samples from 25 sites in selected areas from the different tectonic domains. The AMS is typical for weakly deformed sediments, with a magnetic foliation sub-parallel to the bedding plane, and a well-defined magnetic lineation. The orientation of the magnetic lineation is strongly controlled by the main tectonic deformation recorded in the basins. Structural and AMS data define a transition from NW–SE extension in the Tyrrhenian hinterland domain, to E–W compression in the Catania foredeep domain, to E–W extension in the Hyblean foreland domain, respectively. Reliable paleomagnetic results have been obtained in 12 out of 25 sampled sites. Data show that no significant rotations occurred in any of the studied basins at least since the middle Pleistocene. These results allow us to define an upper limit to the large rotations about vertical axes that have been previously found in the Calabria and Sicily regions.

Keywords: AMS; Paleomagnetism; Plio-Pleistocene; Eastern Sicily

1. Introduction

The study of anisotropy of magnetic susceptibility (AMS) in sediments represents a rapid and valid tool to detect either the depositional processes (Rees, 1965; Schieber and Ellwood, 1988; Kissel et al., 1997) and the deformation pattern related to different tectonic settings (Kissel et al., 1986; Borradaile, 1988; Aubourg et al., 1991; Rochette et al., 1992; Housen et al., 1993; Tarling and Hrouda, 1993; Pares and van der Pluijm, 2002). In undeformed sediments generally the magnetic susceptibility ellipsoid (with $K_1 > K_2 > K_3$) is oblate with the foliation plane (K_1–K_2) that coincides with the bedding plane; this fabric is attributed to depositional and/or compaction processes (Lowrie and Hirt, 1987; Lee et al., 1990; Paterson et al., 1995). If these sediments undergo tectonic deformation, progressively a tectonic AMS subfabric will develop modifying the primary sedimentary magnetic fabric according to the nature and extent of deformation. Several studies have shown that the magnetic fabric can reflect the early stages of deformation (Sagnotti et al., 1994, 1998; Mattei et al., 1999). In such cases K_{max} aligns perpendicular to the shortening direction or parallel to the stretching direction in relation to the existing tectonic regime (Kissel et al., 1986; Mattei et al., 1999 and references therein). In both cases K_{min} remains perpendicular to the bedding plane, still marking the primary magnetic fabric acquired during compaction. Furthermore, the AMS fabric has distinctive character in extensional and compressional tectonic settings (Kissel et al., 1986; Lowrie and Hirt, 1987; Mattei et al., 1997) and, consequently, it constitutes a valid tool in defining the deformative pattern in weakly deformed fine-grained sedimentary sequences, where other classical strain markers are poorly developed or absent.

In eastern Sicily, Plio-Pleistocene sedimentary basins

* Corresponding author.
E-mail address: cifelli@uniroma3.it (F. Cifelli).

0191-8141/03/$ - see front matter © 2003 Elsevier Ltd. All rights reserved.
doi:10.1016/S0191-8141(03)00092-0

related to the foreland, foredeep and hinterland tectonic domains are juxtaposed in a small area. The presence of the Malta escarpment and of the Etna volcano also contributes to the tectonic setting and generates a complicated pattern of Quaternary deformation (Fig. 1). As a consequence, in the last few years a large number of alternative tectonic models have been proposed, which suggest the prevalent role of either the Malta escarpment (Adam et al., 2000), gravitational spreading of the Etna volcano (Borgia et al., 1992, 2000), or regional extensional tectonics related to the Siculo–Calabrian rift (Monaco et al., 1997).

Eastern Sicily thus represents an ideal test site to apply the paleomagnetic approach to unravel the recent structural and tectonic evolution of the region, and to discriminate between the different proposed tectonic models. Magnetic fabric, structural and paleomagnetic studies on Plio-Pleistocene sedimentary sequences exposed in the different tectonic domains of eastern Sicily are combined to obtain insights into the structural architecture and deformation style of each of these domains. The AMS on the relatively undeformed sedimentary deposits is used as a principal tool to detect the deformation pattern in the basins. Where the relationships between sedimentation and faulting are better exposed such information is combined and integrated with structural observations on the brittle deformation features (joints and faults). Integration of such data allows us to describe the recent tectonic evolution of eastern Sicily as occurring into a non-rotational tectonic regime, dominated by NW–SE extension in the Tyrrhenian hinterland domain, by E–W compression in the Catania foredeep domain, and E–W extension in the Hyblean foreland domain.

2. Geological settings

The present day tectonic setting of the Mediterranean region results from the plate convergence between Eurasia and Africa that leads to the formation of a complex pattern of arcuate orogenic belts and extensional back arc basins (Dewey et al., 1989; Horvàth, 1993). The Calabrian Arc and Sicily are examples of this complex geodynamic evolution. During the Neogene, the Calabrian Arc migrated toward the southeast, leading to the opening of the Tyrrhenian back arc basin (Malinverno and Ryan, 1986). The tectonic evolution was mainly controlled by south-eastward roll-back of the subducting Ionian plate, a small fragment of oceanic lithosphere that intervenes between the African continental lithosphere, towards the west, and the Apulian continental lithosphere, towards the east (Malinverno and Ryan, 1986; Faccenna et al., 1997; Catalano et al., 2001) (Fig. 1). In the Calabrian Arc the subduction process is well defined by seismicity (Isacks and Molnar, 1971) and seismic tomographic images (Lucente et al., 1999). In the northern part of the Calabrian Arc, where the subducting plate is oceanic, we observe the largest southeastern displacement of the accretionary wedge. Conversely, in eastern Sicily the orogenic wedge describes a huge syntaxis, corresponding with the location of the Malta escarpment (Fig. 1), which marks the boundary between the present day deforming continental African plate, to the west, and the Ionian oceanic plate to the east, actively subducting below the Calabrian arc (Adam et al., 2000; Nicolich et al., 2000 and references therein) (Fig. 1). In eastern Sicily different structural domains are consequently exposed over a short distance, from south to north: (i) the emerged foreland domain, which outcrops in southern-eastern Sicily and is mostly represented by the Hyblean Plateau; (ii) the orogenic domain, a east- and south-eastward verging thrust belt which includes the Plio-Pleistocene foredeep; and (iii) the hinterland domain, represented by the Tyrrhenian back-arc basin (Lentini et al., 1996).

2.1. The Hyblean foreland domain

The Hyblean Plateau dominates southeastern Sicily (Fig. 1), where it is part of the emerged foreland of the Neogene–Quaternary Maghrebian thrust belt, which was deformed by extensional and strike slip tectonics that are still active (Grasso et al., 1992; Gardiner et al., 1995; Torelli et al., 1998; Monaco and Tortorici, 2000). These fault systems bound and control the development of major Plio-Pleistocene basins such as the Gela–Catania foredeep, located at the western and northwestern edge of the Hyblean Plateau (Fig. 1). Minor basins developed on the Ionian side of the Hyblean Plateau and have been related to the activity on the Malta Escarpment (Grasso and Lentini, 1982; Adam et al., 2000), in a general framework of ESE–WNW regional extension (Tortorici et al., 1995; Monaco and Tortorici, 2000). The Early–Middle Pleistocene sedimentary sequences that fill these depressions are represented by marine sediments distributed along the border of the Hyblean Plateau and become progressively thicker to the north (Torelli et al., 1998).

The study area (Fig. 2) corresponds to the northeastern part of the Hyblean plateau, where Quaternary basins occur along NW–SE-trending tectonic depressions, controlled by normal fault segments such as the Mt Climiti fault. This fault system bounds the Floridia and Augusta basins (Fig. 2), which are filled by a Lower–Middle Pleistocene sequence of basal biocalcarenites, capped by 200–300-m-thick clays and marly clays (Di Grande and Raimondo, 1982). This sequence is unconformably covered by Upper Pleistocene calcarenites (Bordonaro et al., 1984). Several strands of marine terraces developed on top of this sequence on both the tectonic depressions and ridges, which indicates that this area underwent uplift since at least the Middle Pleistocene (Hirn et al., 1997; Bianca et al., 1999). The NW–SE-trending extensional fault system interferes with the younger roughly NNW–SSE-trending normal fault segments recognized in the Ionian offshore zone. This extensional fault system mostly develops in the thinned

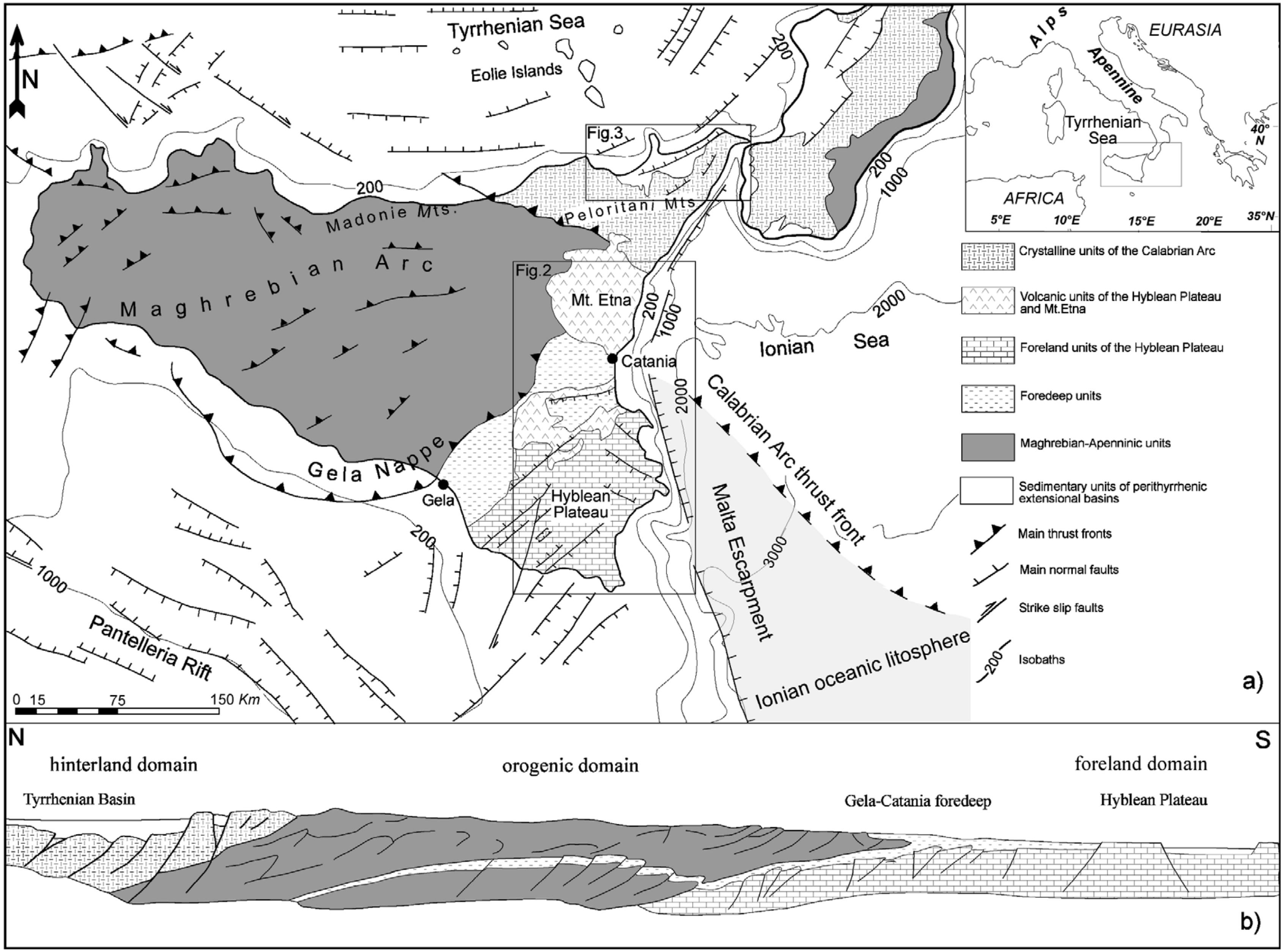

Fig. 1. (a) Schematic map of Sicily and its surrounding areas showing the main structural features (modified after Gardiner et al., 1995); the boxed areas include the study zones. (b) Schematic profile crossing the main structural domains in eastern Sicily (from Lentini et al., 2000).

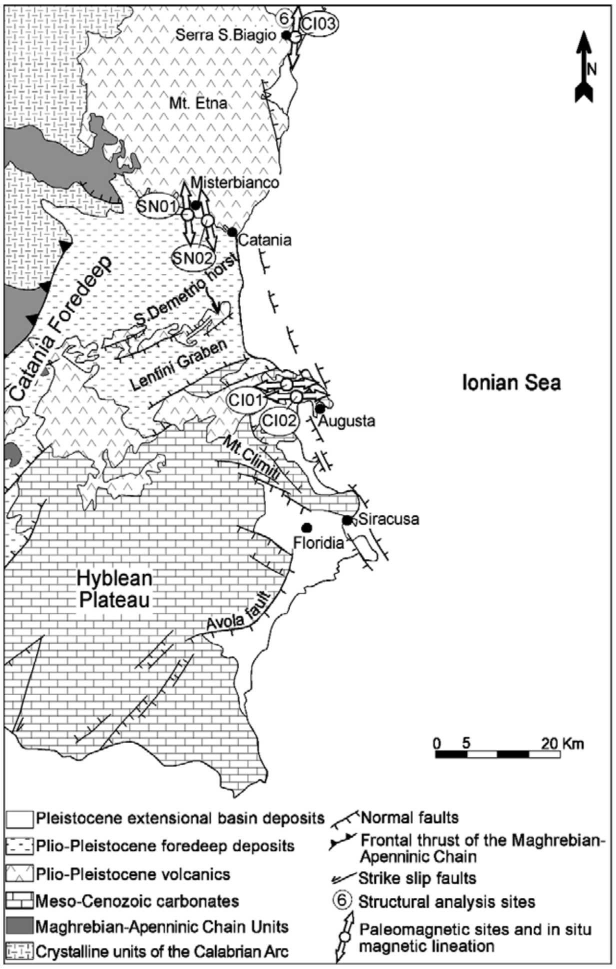

Fig. 2. Schematic geological map of SE Sicily showing the main tectonic features of the region and location of paleomagnetic sites. (For the location of area see Fig. 1.) Fault pattern after Bianca et al. (1999) and references therein.

crust of the Ionian domain reactivating the Malta Escarpment south of Augusta (Bianca et al., 1999).

2.2. The foredeep domain

The foredeep domain flanks the collapsed margin of the Hyblean Plateau and runs from Catania to Gela (Fig. 1). It is a SW–NE-trending, narrow and weakly deformed depression. In the study area the foredeep domain corresponds to the Catania foredeep basin (Fig. 2); the transition between the northern part of the Hyblean Plateau and this area is related to a NE–SW-trending normal fault system, which defines the Lentini Graben and the San Demetrio Horst. Sediments in the basin are represented by biocalcarenites, which outcrop in the structural highs that grade into blue marly and silty clays in the depressions (Torelli et al., 1998).

From the southern border of the Mt. Etna volcano to the Ionian coast, the foredeep deposits are made up of a succession of bluish silty–marly clays up to 600 m thick with rare intercalation of yellowish fine-grained sands, that grade upward to some tens of meters of sands and conglomerates. The marly clays, which are affected by compressional structures, contain fauna indicating a Lower–Middle Pleistocene age (Wezel, 1967; Di Stefano and Branca, 2002). However, the tholeiitic composition of the volcanic clasts, contained in the conglomeratic levels (Monaco, 1997), indicates that the age of sands and conglomerates are related to the early stage of the Etnean volcanic activity (Romano, 1982), dated 365–235 ka in the area to the west of Catania (Gillot et al., 1994). As the sands and conglomerates are, in turn, covered by tholeiitic lava flows west of Catania, their age is thus constrained between 365 and 235 ka. Terraced deposits overlie unconformably the sediments of the Lower–Middle Pleistocene cycle at different elevations. They form coastal sedimentary wedges that pinch landwards (Bosi et al., 1996), with thin alluvial and/or colluvial caps and basal contacts usually marked by erosional surfaces and levels of paleosoils.

In the Catania foredeep basin the deformation history of the Quaternary sediments was previously studied by means of fault slip analysis along the southern margin of Mt. Etna (Labaume et al., 1990). These results indicated a multistage deformation history, deduced from syn-sedimentary folding, and subsequent eastward-directed brittle shear, which is related to a compressional event. On the other hand, Borgia et al. (1992, 2000) interpreted this deformative pattern as related to gravitational spreading of the Etna volcano, which should produce extensional structures in the summit region of Mt. Etna and radial compressive structures at the base of the volcano.

2.3. The hinterland domain

The northern Sicily continental margin has been affected by shortening and thrusting during the Tertiary formation of the Sicilian–Maghrebian and Kabilian–Calabria fold-and-thrust belts (Catalano et al., 1985). Widespread normal faulting, clearly imaged by seismic data, demonstrates, however, the importance of thinning and extensional processes in the tectonic evolution from Neogene to Recent (Lentini et al., 1995; Pepe et al., 2000). The age of inception of extensional tectonics in this area is still debated, and has been proposed to be Serravallian (Lentini et al., 1995) or late Tortonian times (Catalano et al., 1996; Pepe et al., 2000). According to Lentini et al. (1995), extensional tectonics is accompanied by the deposition of thick sedimentary sequences, starting with Serravallian siliciclastic deposits. The Lower Pliocene Trubi Formation represents a marine transgressional phase that, following the Messinian salinity crisis, re-established the marine environment at normal salinity over a large area, previously characterized by emersion or deposition of evaporites (Catalano et al., 1996). These units are overlain by Upper Pliocene–Middle Pleistocene transgressive sequences, characterized by a gradual vertical transition from calcarenites to sands and clays. Finally, since the Middle

Pleistocene the entire northern Sicilian hinterland domain underwent a strong regional uplift (Catalano and Di Stefano, 1997; Bordoni and Valensise, 1998).

The investigated area in this study extends from Capo Tindari to Villafranca Tirrena (Figs. 1 and 3). The structural architecture of this region is mainly controlled by NE–SW-trending major fault systems. This system is intersected by NW–SE oriented steeply-dipping fault strands, which are orthogonal to the main 'Tyrrhenian' structural trend (Lentini et al., 2000).

3. Sampling and laboratory methods

We sampled 329 oriented cylindrical samples from 25 sites in different tectonic units. Two sites were sampled in the foreland Augusta Basin (CI01, CI02) on the Hyblean Plateau (Fig. 2); three sites in the Catania foredeep basin (CI03, SN01 and SN02) (Fig. 2) and 20 sites were located in the hinterland domain of the Tyrrhenian Peloritani margin (Fig. 3). Sixteen sites were sampled in the Middle–Pleistocene clays; seven sites in the Lower Pliocene Trubi Formation, the latter only in the hinterland domain, where also two sites were sampled in Serravallian marls.

At each site, cores were drilled with an ASC 280E petrol-powered portable drill and oriented in situ by a magnetic compass. From each core one to three standard (25 mm diameter × 22 mm height) cylindrical specimens were cut.

Most of the magnetic measurements were carried out at the paleomagnetic laboratory of the Department of Geological Sciences of the "Roma Tre" University. Measurements on a Princeton Measurement Corporation vibrating sample magnetometer (VSM) and AF demagnetization were performed at the paleomagnetic laboratory of the Institute of Geophysics (ETH) in Zurich.

The nature of the magnetic carriers was investigated for one sample from each site, using different rock magnetic techniques. The stepwise acquisition of an isothermal remnant magnetization (IRM) was carried out using a pulse magnetizer to apply magnetic fields up to 2 T. The coercivity of remanence (B_{cr}) was then estimated by stepwise application of a back-field up to 2 T to remove the forward-field of 2 T IRM. In order to discriminate the ferrimagnetic mineralogy, we also applied 0.12, 0.6 and 1.7 T fields along the three orthogonal specimen axes and the three-component IRM was subsequently thermally demagnetized (Lowrie, 1990). The relative contributions of the paramagnetic clay matrix and the ferrimagnetic minerals to the magnetic susceptibility were evaluated by measuring hysteresis properties in one sample per site using a VSM. The low-field magnetic susceptibility for one specimen from each core was measured with an AGICO KLY-3 bridge and the AMS at both the specimen and the site levels was evaluated using Jelinek statistics (Jelinek, 1977, 1978). The NRM (natural remnant magnetization) of the samples was analysed both by means of progressive stepwise thermal demagnetization using small temperature increments (30–50 °C) and stepwise alternating field demagnetization. Data were analyzed using orthogonal vector diagrams and directions of the remanence components were estimated using principal component analysis (Kirschvink, 1980).

4. Magnetic mineralogy

Low coercivity ferrimagnetic minerals were identified in most of the clay sites (Fig. 4a and b). In three sites (CI04, SN03, SN15) the maximum unblocking temperature spectra is in the range of 320–360 °C, which suggests that the magnetic mineralogy is dominated by iron sulphides (Fig. 4c). Furthermore, these sites display high saturation isothermal remnant magnetization (SIRM) to low field magnetic susceptibility (K) ratios ($SIRM/K > 10$ kA/m), and hysteresis ratios typical for the single domain grains ($M_{rs}/M_s > 0.5$ and $(B_o)_{cr}/(B_o)_c > 1.5$, where M_{rs} is the saturation remanence, M_s is the saturation magnetization, $(B_o)_c$ is the coercive force and $(B_o)_{cr}$ is the coercivity of remanence. The combination of unblocking temperature and magnetic ratios suggests that greigite (Fe_3S_4) is the dominant ferrimagnetic phase, although the presence of pyrrhotite cannot be precluded (Roberts, 1995; Sagnotti and Winkler, 1999).

In other clay sites (CIO3, SN02, SN10, SN14), the maximum unblocking temperature is about 580 °C, which indicates magnetite as the main magnetic carrier (Fig. 4d). All the other clay sites display intermediate behavior, suggesting the presence of magnetite associated with iron sulphides.

In contrast, high-coercivity magnetic carriers were identified at most of the sites in the Trubi Formation (Fig. 4a and b). In these sites (SN09, SN11, SN12 and SN16) the multi-component IRM is characterized by the prevalence of medium and hard coercivity fraction (above 0.6 T) with a maximum unblocking temperature of about 600 °C, indicating hematite as a main magnetic carrier (Fig. 4e).

The mean magnetic susceptibility (K_{mean}) values range between 30 and 75×10^{-6} SI (Fig. 5a and Table 1) for the Pliocene marls, and between 100 and 500×10^{-6} SI (Fig. 5b and Table 1) for the clays. In site CI04 K_{mean} reaches up to 1180×10^{-6} SI. These susceptibility values confirm the different magnetic mineralogy of marls and clays, also suggesting a significant contribution of iron-sulphides to the clay magnetic mineralogy.

Hysteresis properties were also measured in one sample per site in order to estimate quantitatively the ferrimagnetic versus the paramagnetic contribution to the low-field susceptibility. All the sites from the Trubi formation (SN08, SN09, SN11, SN12, SN16, SN17 and SN18) show a typical paramagnetic behavior (Fig. 5c). In contrast, clay sites show different behavior. In CI01, CI05, SN06, SN07 and SN13 sites, a small hysteresis loop is observed,

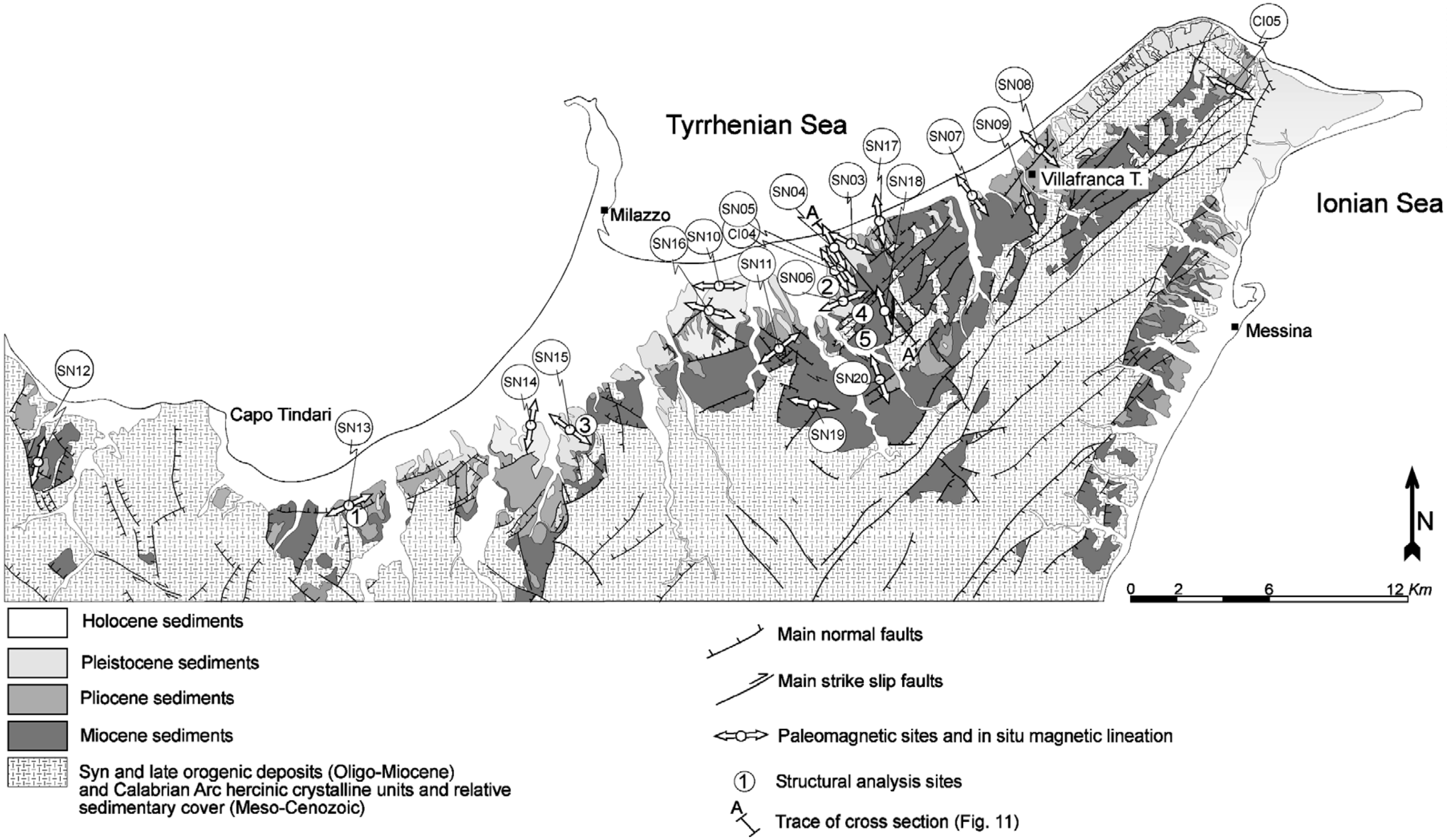

Fig. 3. Geological setting of the northern margin of the Peloritani Mountains (modified after Lentini et al., 2000) and location of sampling and structural analysis sites. (For the location of the area see Fig. 1.)

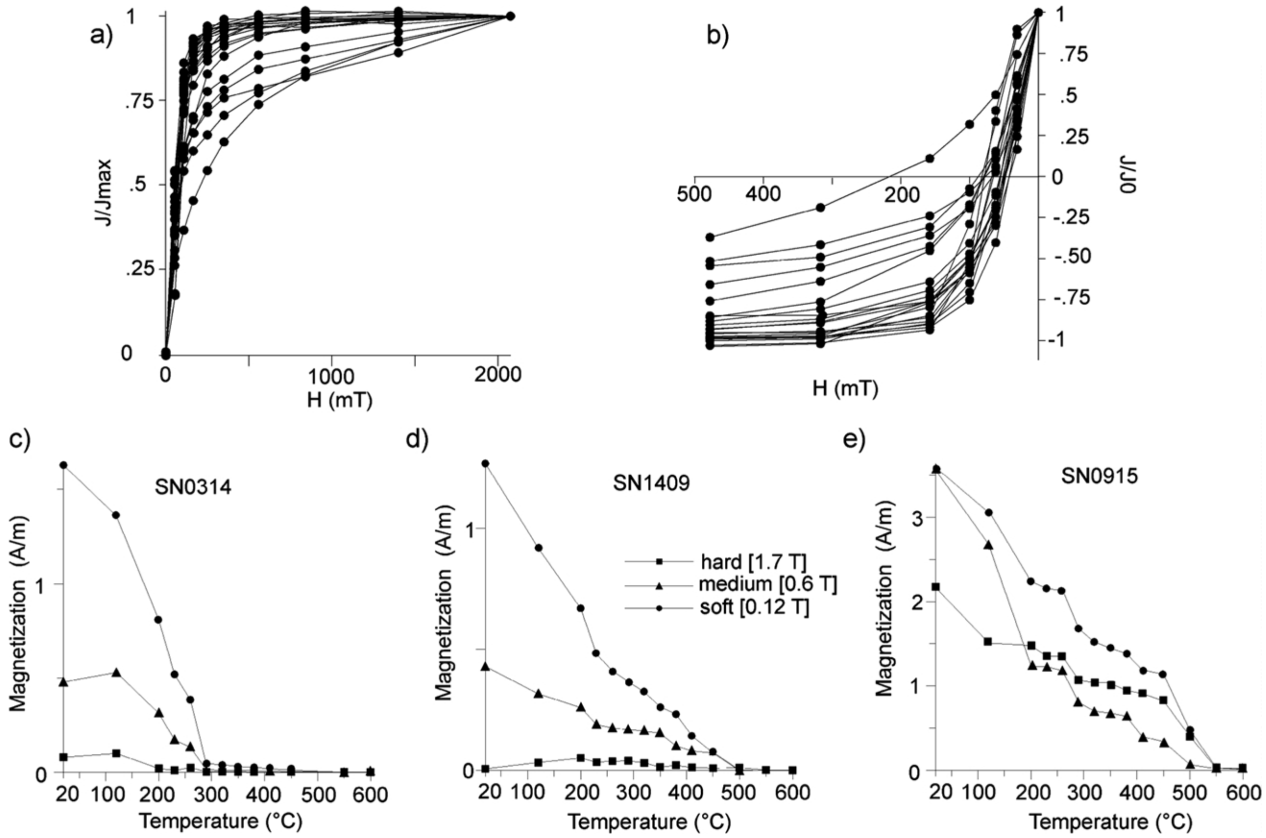

Fig. 4. IRM (a) and HCR (b) acquisition curves for all the examined sites. Thermal demagnetization of a composite IRM produced sequentially in fields of 1.7, 0.6 and 0.12 T for samples from sites SN03 (c), SN14 (d) and SN09 (e).

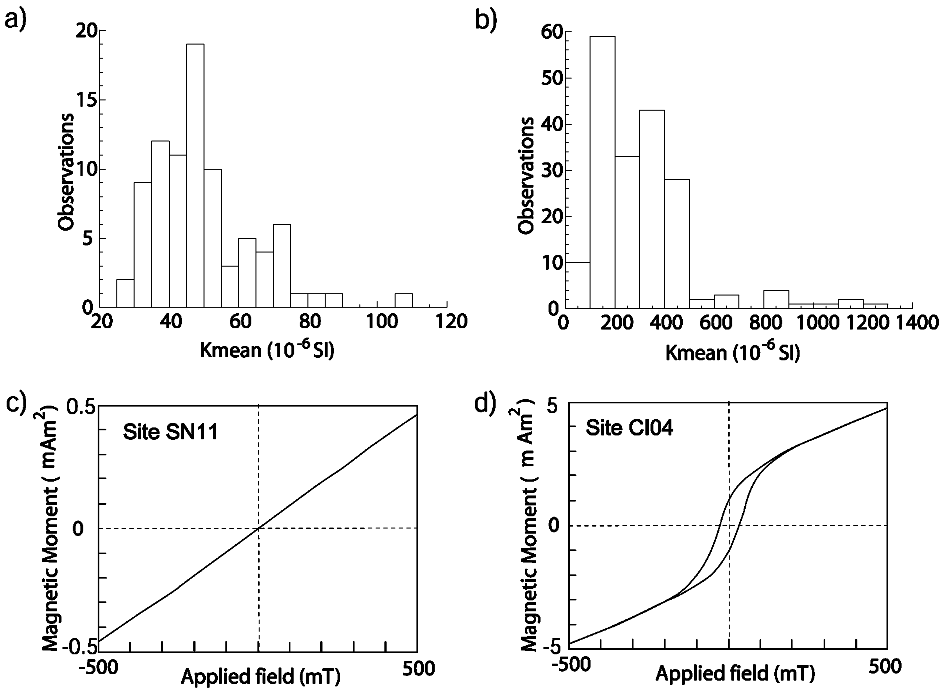

Fig. 5. Frequency distribution of the mean susceptibility (K_{mean}) values in the marls of Trubi Formation (a) and in the clays (b). Hysteresis loops measured for marl samples (c) (no ferrimagnetic contribution to the susceptibility) and for clay samples (d) (significant ferrimagnetic contribution to the susceptibility).

Table 1
List of anisotropy factors computed at each site

Site	Lithology	N	k_m	L	F	Pj	Tj	S_0	D, I (K_{min})	D, I (K_{max})	E_{1-2}
CI01	Clays	11	173.8 (15.0)	1.003 (0.001)	1.019 (0.002)	1.024 (0.003)	0.762 (0.096)	116, 6	296, 84	266, −5	32
CI02	Clays	7	134.5 (7.4)	1.002 (0.001)	1.007 (0.002)	1.009 (0.001)	0.486 (0.235)	0, 0	216, 51	88, 26	27
CI03	Clays	11	392.2 (51.3)	1.015 (0.004)	1.020 (0.002)	1.036 (0.004)	0.154 (0.138)	214, 31	99, 41	5, 4	3
CI04	Clays	11	788.6 (272.6)	1.013 (0.008)	1.045 (0.018)	1.061 (0.025)	0.563 (0.170)	Variable	173, 80	328, 9	18
CI05	Clays	9	93.0 (3.2)	1.005 (0.001)	1.032 (0.005)	1.040 (0.006)	0.743 (0.065)	0, 0	324, 86	297, −4	29
SN01	Clays	5	217.3 (9.8)	1.005 (0.001)	1.023 (0.005)	1.030 (0.005)	0.631 (0.080)	30, 10	157, 70	174, 15	13
SN02	Clays	5	236.4 (11.6)	1.009 (0.002)	1.022 (0.009)	1.032 (0.009)	0.376 (0.287)	340, 15	118, 78	347, 8	26
SN03	Clays	8	373.9 (71.3)	1.012 (0.004)	1.064 (0.014)	1.083 (0.019)	0.687 (0.068)	0, 0	270, 87	297, −3	9
SN04	Clays	10	235.2 (47.7)	1.005 (0.003)	1.033 (0.007)	1.041 (0.009)	0.766 (0.131)	91, 43	270, 50	334, −20	25
SN05	Clays	12	481.9 (281.1)	1.006 (0.004)	1.040 (0.005)	1.050 (0.009)	0.732 (0.161)	301, 15	334, 79	324, −11	35
SN06	Clays	9	179.7 (33.9)	1.014 (0.006)	1.050 (0.007)	1.069 (0.010)	0.557 (0.154)	0, 0	240, 78	69, 12	39
SN07	Marls	11	177.8 (9.5)	1.005 (0.002)	1.050 (0.009)	1.062 (0.012)	0.804 (0.048)	0, 0	220, 78	323, 3	20
SN08	Marls	10	37.5 (6.2)	1.008 (0.005)	1.011 (0.002)	1.019 (0.006)	0.245 (0.319)	0, 0	37, 66	314, −3	53
SN09	Clays	13	39.2 (3.5)	1.005 (0.005)	1.005 (0.003)	1.010 (0.007)	0.115 (0.397)	0, 0	39, 77	343, −7	28
SN10	Clays	15	428.6 (125.7)	1.007 (0.003)	1.040 (0.007)	1.051 (0.008)	0.701 (0.116)	0, 0	48, 88	271, 1	12
SN11	Marls	14	51.0 (4.8)	1.005 (0.006)	1.009 (0.006)	1.015 (0.012)	0.401 (0.272)	125, 30	307, 64	54, 8	40
SN12	Marls	14	70.8 (7.5)	1.003 (0.003)	1.017 (0.002)	1.022 (0.003)	0.725 (0.236)	60, 15	255, 58	16, 18	21
SN13	Clays	14	112.0 (7.3)	1.005 (0.001)	1.010 (0.002)	1.015 (0.003)	0.382 (0.100)	0, 0	116, 62	66, −19	9
SN14	Clays	11	221.8 (28.5)	1.004 (0.002)	1.031 (0.005)	1.039 (0.006)	0.761 (0.094)	182, 16	359, 77	11, −13	29
SN15	Clays	9	342.9 (71.9)	1.008 (0.003)	1.027 (0.004)	1.037 (0.003)	0.526 (0.165)	250, 9	269, 85	307, −4	10
SN16	Marls	14	46.6 (4.3)	1.011 (0.002)	1.007 (0.003)	1.018 (0.002)	−0.238 (0.261)	0, 0	228, 72	107, 10	10
SN17	Marls	12	49.7 (25.7)	1.028 (0.024)	1.033 (0.101)	1.121 (0.132)	0.343 (0.269)	0, 0	203, 72	352, 15	40
SN18	Marls	8	50.7 (4.6)	1.003 (0.001)	1.004 (0.001)	1.008 (0.002)	0.213 (0.202)	0, 0	72, 58	344, −2	30
SN19	Marls	10	197.2 (10.3)	1.015 (0.002)	1.046 (0.004)	1.065 (0.005)	0.502 (0.045)	0, 0	22, 45	101, 11	15
SN20	Marls	9	208.0 (11.5)	1.006 (0.002)	1.053 (0.006)	1.066 (0.007)	0.791 (0.068)	0, 0	71, 34	340, 7	19

N = number of specimens; $k_m = (k_{max} + k_{int} + k_{min})/3$ (mean susceptibility, in 10^{-6} SI units); $L = k_{max}/k_{int}$; $F = k_{int}/k_{min}$; $Pj = \exp\{2[(\eta 1 - \eta)^2 + (\eta 2 - \eta)^2 + (\eta 3 - \eta)^2]\}^{1/2}$ (corrected anisotropy degree; Jelinek, 1981); $Tj = 2(\eta 2 - \eta 3)/(\eta 1 - \eta 3) - 1$ (shape factor; Jelinek, 1981); S_0 = bedding attitude (azimuth of the dip and dip values); $\eta 1 = \ln k_{max}$; $\eta 2 = \ln k_{int}$; $\eta 3 = \ln k_{min}$; $\eta = (\eta 1 + \eta 2 + \eta 3)/3$; E_{1-2} = semi-angle of the 95% confidence ellipses around the principal susceptibility axes. For each locality the line shows the arithmetic means of the individual site mean values (standard deviation in parentheses).

indicating a possible small contribution of ferrimagnetic minerals to the magnetic susceptibility. In the remaining examined sites (CI03, CI04, SN03, SN04, SN05, SN10, SN14 and SN15), the ferrimagnetic contribution seems to be significant with an open hysteresis loop (Fig. 5d); in these sites iron-sulphides have been generally identified.

5. AMS results

The measurement of the low-field anisotropy of magnetic susceptibility (AMS) represents a cheap, rapid and non-destructive technique for the characterization of the mineral fabric of rocks (Hrouda, 1982). AMS is defined by a second rank tensor and represented geometrically by an ellipsoid in which the greatest intensity of magnetization is induced along the long axis K_{max} and the weakest intensity along the short axis K_{min} (with principal axes $K_{max} > K_{int} > K_{min}$).

Several parameters have been defined both for the quantification of the magnitude of anisotropy and for defining the shape of the ellipsoid (see Table 1; Jelinek, 1981; Hrouda, 1982). The magnetic lineation L (K_{max}/K_{min}) is defined by the orientation of K_{max}, while the magnetic foliation F (K_{int}/K_{min}) is defined as the plane perpendicular to K_{min}. The anisotropy degree is expressed by the parameter Pj (Jelinek, 1981).

In eastern Sicily, all the examined sites (clays and marls) have AMS parameters typical for weakly deformed sediments, with Pj values less than 1.12 (Fig. 6a and Table 1), and oblate to triaxial ellipsoid shapes (i.e. $F \gg L$; Fig. 6b and Table 1). The L parameter has a small range of values within all the sampling sites (site SN17 was not considered), regardless of the magnetic mineralogy ($1.003 < L < 1.015$ for the clays and $1.003 < L < 1.011$ for the marls). On the other hand, a larger variation of F is noted for the clays, suggesting that both the paramagnetic and ferrimagnetic minerals contribute to the susceptibility anisotropy. In particular, the sites that exhibit the largest mean F values are characterized by the presence of iron-sulphides and have the highest values of K_{mean}. In summary, the magnetic fabric for most of the sites is well defined and both magnetic foliation F and magnetic lineation L are observed (Table 1 and Fig. 7).

In the Augusta area (foreland domain) the two sites (CI01 and CI02), both sampled in Pleistocene clay units, exhibit similar fabrics. The magnetic foliation is sub-parallel to the bedding plane and shows a well-defined magnetic lineation with a mean E–W orientation (Fig. 7a).

In the Catania area (foredeep domain), the Pleistocene clay sites (CI03, SN01 and SN02), exhibit a quite shallow-dipping magnetic foliation and a consistent magnetic

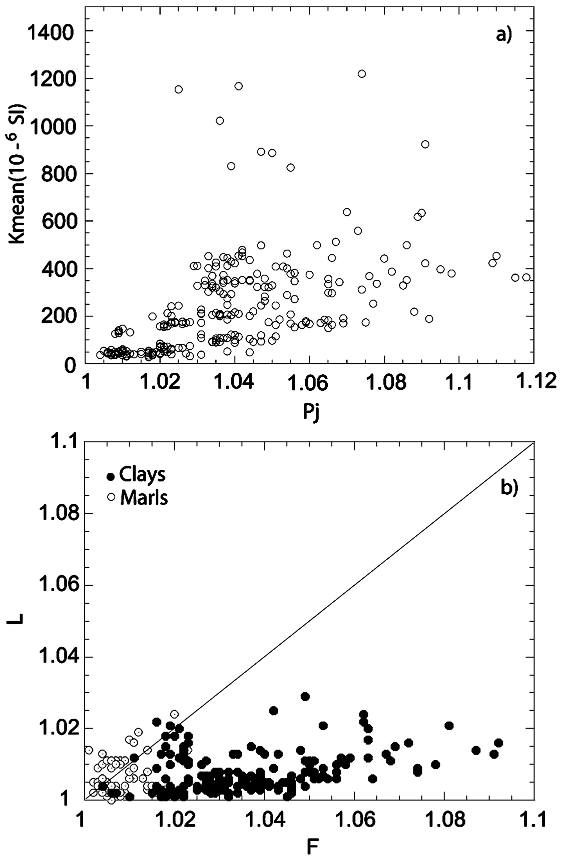

Fig. 6. (a) Degree of anisotropy Pj vs. mean susceptibility $K_{mean.}$; (b) F–L plot for all the samples investigated in this study: white and dark gray spots represent marl and clay samples, respectively.

lineation that is N–S to NNW–SSE in trend (Fig. 7b and Table 1).

In the hinterland domain, the magnetic foliation is sub-parallel to the bedding plane. The magnetic lineation trends NNW–SSE to WNW–ESE (Fig. 7c and d) in most of the sites (CI04, CI05, SN03, SN04, SN05, SN07, SN08, SN09, SN15, SN16, SN17, SN18, SN19, SN20). Sites SN06, SN11, SN12 and SN13 are characterized by a magnetic lineation oriented ENE–WSW, site SN10 has E–W oriented magnetic lineation, and site SN14 shows a N–S magnetic lineation (Table 1).

Several studies show that, when the magnetic lineation is controlled by the paleoflow, K_{max} generally extend over a wide range of azimuths, both within a single layer and throughout a stratigraphic sequence, corresponding to temporal changes of the flow direction within the basin (Hamilton and Rees, 1970; Hailwood and Sayre, 1979; Kissel et al., 1997). On the contrary, in all the sites we measured, the trend of the magnetic lineation is maintained through sequences that differ in sedimentological characters and age. Furthermore, a correlation between the orientation of the brittle deformation pattern and the magnetic lineations has been systematically noted. These observations support a tectonic origin of the magnetic lineation.

6. Paleomagnetic results

The natural remnant magnetization (NRM) of the samples was analyzed both by means of progressive stepwise thermal demagnetization and alternating field demagnetization. Thermal demagnetization is usually better in isolating the components of magnetization in the marine marls and clays (Ouliac, 1976). The thermal demagnetization technique, however, may cause possible mineral alterations, especially at high temperatures, that may lead to the production of new ferrimagnetic phases.

The NRM was measured using an AGICO JR5-A spinner magnetometer. Samples were thermally demagnetized with small temperature increments (30–50 °C). AF demagnetization was done incrementally up to 120 mT, using a 2G cryogenic magnetometer in the shielded room of the paleomagnetic laboratory of the Institute of Geophysics (ETH) in Zurich. Similar results for AF and thermal demagnetization were obtained on sister samples from the same cores. Magnetic cleaning treatment was stopped when NRM decreased to the limit of the instrument sensitivity or when random changes of the paleomagnetic directions appeared.

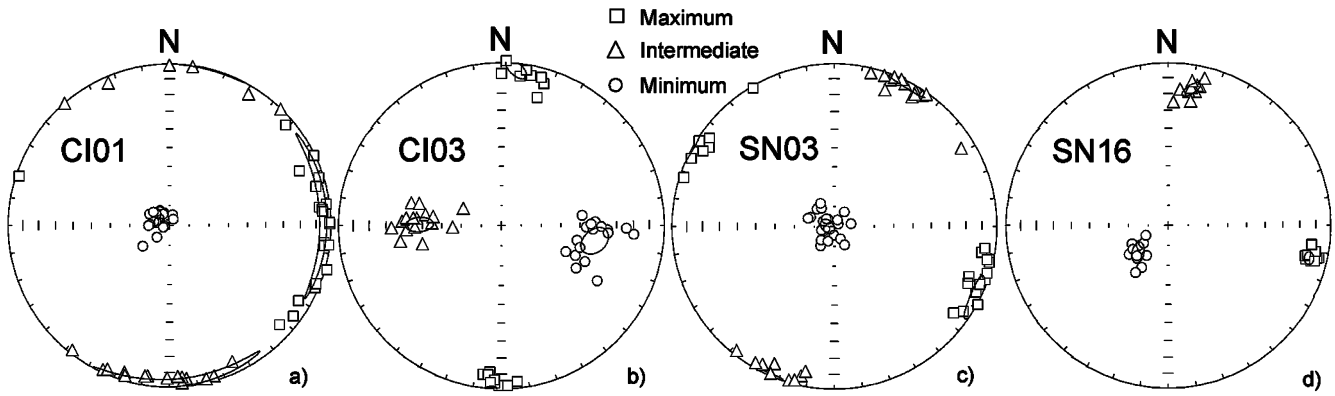

Fig. 7. AMS results from the most significant investigated sites plotted on equal area, lower hemisphere projections. (a) Augusta area (foreland domain); (b) Catania Plain (foredeep domain); (c) and (d) Northern margin of the Peloritani Mountains (back arc domain).

The NRM at seven sites (CI02, CI05, SN07, SN10, SN13, SN19 and SN20) was found to be too weak (NRM $< 10^{-5}$ A/m) or unstable after the first demagnetization steps. These sites were excluded from further paleomagnetic evaluation.

In most of the remaining clay samples a characteristic remanent magnetization (ChRM) has been isolated after the removal of a small viscous component of magnetization. Most of the sites were completely demagnetized at 300–350 °C or at 550–580 °C, confirming iron-sulphides and/or magnetite as the carriers of remanence (Fig. 8). Site-mean directions were obtained using Fisher (1953) statistics where stable components of magnetization were isolated and McFadden and McElhinny's method (1988) was applied to data fitted with great circles (Table 2). The mean directions are well defined for most of the sites and α_{95} rarely exceeds 10°. The mean ChRM for all the clay sites is $D = 360.0°$; $I = 47.9°$; $K = 30.3$; $\alpha_{95} = 10.8°$, which indicates that no significant rotation occurred in eastern Sicily since the middle Pleistocene. After bedding correction, all the sites have northward declination (normal polarity). The data show a positive fold test at 99% confidence level ($\xi_{\text{in situ}} = 4.88$; $\xi_{\text{unfolded}} = 3.88$; $\xi_{99\%} = 5.62$) (McFadden, 1990). This indicates both satisfactory magnetic cleaning and the primary nature of the ChRM.

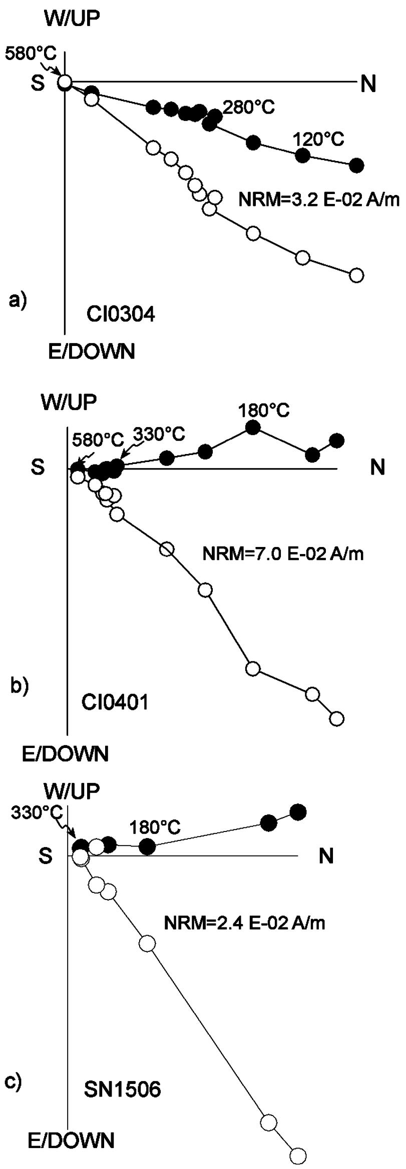

Fig. 8. Vector component diagrams for the progressive thermal demagnetization of samples from clay deposits. Demagnetization step values are in degrees Celsius. Open and solid symbols represent projection on the vertical and horizontal planes, respectively.

Sites from Trubi Formation were sampled only in the Tyrrhenian margin of the Peloritani Mountains. Marls of the Trubi Formation have generally weak NRM and show unstable results in both thermal and AF demagnetization, as observed in other paleomagnetic studies on these rocks (Grasso et al., 1987; Scheepers and Langereis, 1994; Speranza et al., 1999). It is difficult to remove the secondary component of magnetization that overprint the primary component, which is thought to be of chemical origin, acquired immediately after deposition or during the diagenesis (Grasso et al., 1987). For this reason, it was not possible to isolate the primary paleomagnetic direction in six of the seven analyzed sites. Only SN12 gave reasonable results (Table 2) and was used for tectonic evaluation. This site has a reversed polarity with mean ChRM $D = 177.3°$; $I = -50.2°$; $K = 58.4$; $\alpha_{95} = 7.0°$, which is almost antipodal to the mean of the normal polarity clay sites. The McFadden (1990) fold test, however, is indeterminate.

7. Structural data

Structural data were collected in the foredeep and in the hinterland domains, where brittle deformative features were recognizable at outcrop scale. Conversely, no visible deformation was observed in the clay sequences of the foreland domain, exposed in the Augusta area. Consequently, the deformation pattern of these clay sequences was investigated exclusively by means of AMS.

7.1. Hinterland domain

The main deformation recognized along the northern shoulder of the Peloritani chain consists of NE–SW-trending extensional faulting of regional importance. The NE–SW main extensional trend is locally segmented by N–S- to NW–SE-trending fault strands with extensional to transtensional kinematics (Fig. 3).

The NE–SW extensional fault systems that affect the Mio-Pliocene and Pleistocene deposits show consistent NW–SE-trending slickenlines. The general architecture of the overall fault arrays can be adequately described in terms of domino faulting with a mean dip towards the NW (e.g. Wernicke and Burchfield, 1982).

Table 2
Paleomagnetic directions from eastern Sicily

Site	Age	*N*1, *N*2/*N*	Dbtc (°)	Ibtc (°)	α_{95} (°)	Datc (°)	Iatc (°)	*k*	α_{95} (°)	S_0 (°)
CI01	Middle Pleist.	2, 6/8	5.8	40.9	9.9	10.90	42.80	37.58	9.9	116, 6
CI03	Middle Pleist.	10, 0/10	14.5	34.8	5.0	357.50	62.60	95.25	5.0	214, 31
CI04	Middle Pleist.	10, 1/11	30.3	55.0	16.5	14.60	45.60	30.81	8.1	Variable
SN01	Middle Pleist.	5, 0/5	353.4	38.7	8.1	357.33	30.46	89.80	8.1	30, 10
SN02	Middle Pleist.	1, 5/6	356.7	62.9	16.7	351.40	48.40	23.26	16.7	340, 15
SN03	Middle Pleist.	14, 0/14	16.7	45.3	3.3	16.70	45.30	144.97	3.3	0, 0
SN04	Middle Pleist.	11, 2/13	332.2	53.9	5.9	34.60	51.70	50.16	5.9	91, 43
SN05	Middle Pleist.	13, 0/13	358.2	46.4	5.0	347.60	37.10	68.42	5.0	301, 15
SN06	Middle Pleist.	1, 3/4	348.30	40.2	22.0	348.30	40.20	33.17	22.0	0, 0
SN10*	Middle Pleist.	3, 7/10	241.5	−77.7	11.0	241.50	−77.70	22.24	11.0	0, 0
SN12	Early Pliocene	5, 4/9	158.5	−54.9	7.0	177.33	−50.20	58.44	7.0	60, 15
SN14	Middle Pleist.	5, 4/9	343.4	47.1	9.9	335.00	60.10	32.52	9.9	182, 16
SN15	Middle Pleist.	10, 1/11	355.5	49.7	4	344.70	50.80	150.9	4	250, 9

Mean for all the sites but SN10 ($N = 12$): before tectonic correction $D = 358.2°$; $I = 48.5°$; $k = 35.6$; $\alpha_{95} = 7.4°$ after tectonic correction $D = 359.8°$; $I = 48.1°$; $k = 33.2$; $\alpha_{95} = 7.6$. *N*1, *N*2/*N* number of stable directions, number of great circles/total number of studied samples at a site. *D*, *I* site mean declinations and inclinations calculated before (Dbtc, Ibtc) and after (Datc, Iatc) tectonic correction. *k* and α_{95}, statistical parameters after Fisher (1953). S_0 bedding attitude (azimuth of the dip and dip values).

The main NE–SW-trending fault planes are shallow to moderate dipping (from 15 to 40°), with centimeter width fault cores (Fig. 9). Accordingly, the faulted sedimentary strata are tilted towards the southeast, with a mean dip of 15–20°. An overall thickening of the sedimentary strata can be observed approaching the major fault planes (Fig. 9a), which attests to their syn-sedimentary activity. Antithetic fault systems are systematically steeply dipping, with dip angles from 60 to 80°. Extensional conjugate systems are often developed at the hanging wall of the major north-westward-dipping extensional faults. Southeastward rotated (antithetic with shear) conjugate systems are observed with southeastward steeply dipping fault planes (80° to vertical). Also unrotated conjugate systems occur, with dips on the order of 60–70°, thus roughly compatible with ≪ Andersonian ≫ conjugate shear in an extensional setting (e.g. Price and Cosgrove, 1990). The deformation pattern is completed with the occurrence of steeply dipping ENE–WSW-trending fracture arrays in less deformed shear lenses (Fig. 10). A cross-section normal to the main NE–SW structural trend reveals that extensional block faulting controls the present tectonic setting of the area, with normal offset increasing as one moves towards the coast (Fig. 11). The Mio-Pliocene sequences show a similar deformation pattern along the cross-section as described above. Conjugate NE–SW-trending extensional faults and similarly oriented steeply dipping fractures bisect the dihedral angle between the conjugate fault systems. Fault population analysis indicates a general NW–SE-trending maximum extension direction for both the Pleistocene and Mio-Pliocene sedimentary sequences (Fig. 11).

7.2. Foredeep domain

In the foredeep domain, structural data were collected at the paleomagnetic site CI03 (site 6 in Fig. 2), whereas sites SN01 and SN02 have already been investigated by Labaume et al. (1990). At site CI03, fault surfaces are scarce and slickensided surfaces are poorly preserved. Fault systems consists of roughly N–S-trending reverse faults. When present, slickenlines on polished fault surfaces are E–W-trending. Compressional deformation at site CI03 thus records a mean E–W-trending shortening direction, in agreement with the N–S oriented magnetic lineation (Fig. 12). Such data are in agreement with those of Labaume et al. (1990), derived from the Misterbianco area.

8. Discussion

Integration of the combined AMS, paleomagnetic and structural data can provide first-order constraints on the Plio-Pleistocene tectonic regimes of eastern Sicily, moving from the hinterland domain to the foreland domain, passing through the foredeep domain.

In both the hinterland and foreland domains, magnetic foliation is sub-parallel to the bedding, which suggests a primary sedimentary magnetic fabric (e.g. Graham, 1966; Kissel et al., 1986; Lee et al., 1990; Sagnotti and Speranza, 1993; Scheepers and Langereis, 1994; Mattei et al., 1999). Magnetic lineations in sedimentary rocks can be of depositional or tectonic origin. Based on the arguments given above, a sedimentary origin appears unlikely. On the other hand, the orientation of the magnetic lineations derived from the different sedimentary sequences strictly reflects the main tectonic features of the individual sedimentary basins. The magnetic lineation shows remarkable coherence within each tectonic domain and strongly correlates with the main structural features either in compressional or extensional regimes.

In the hinterland domain a mean NW–SE-oriented direction of extension was inferred from orientation of the

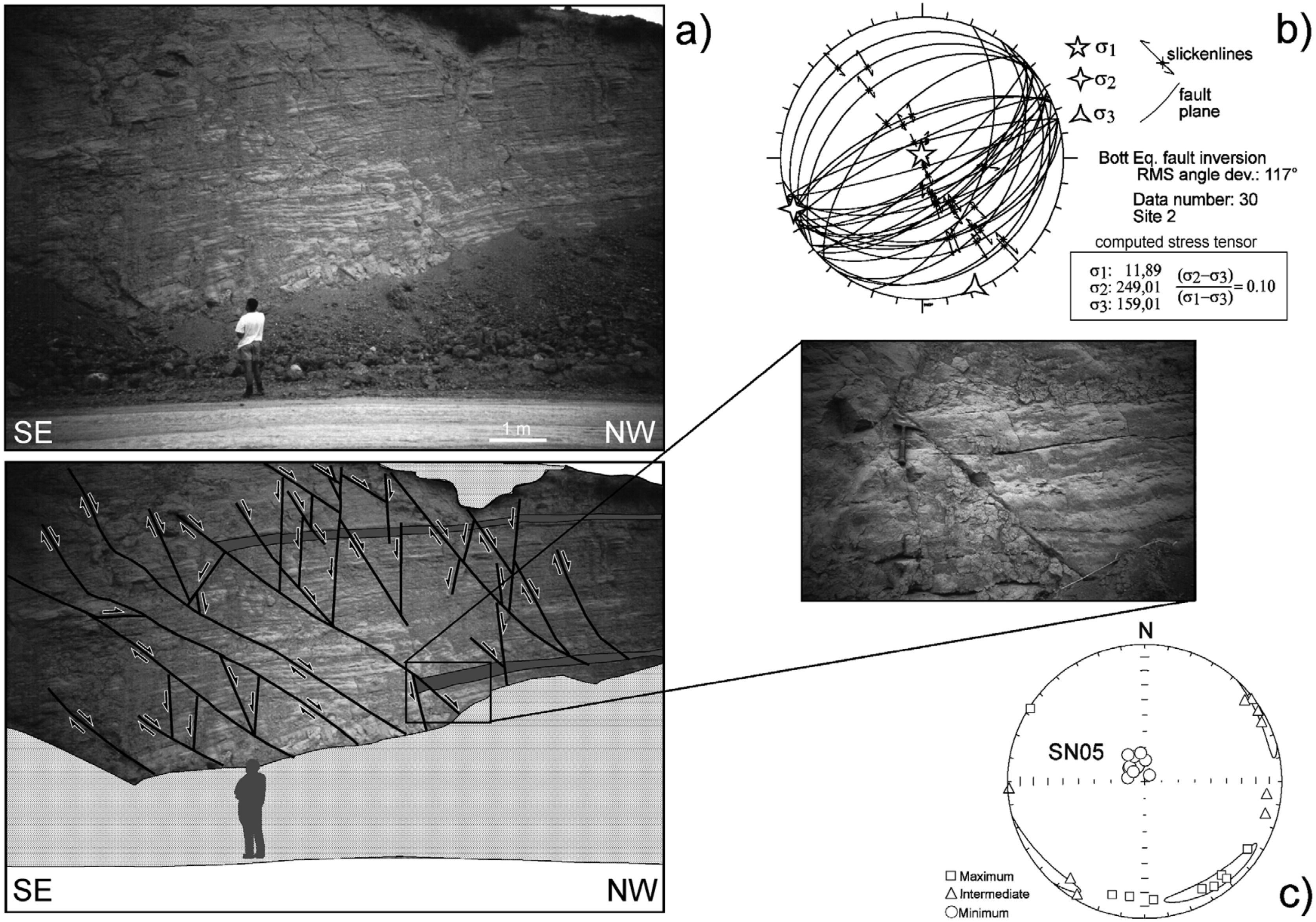

Fig. 9. Brittle deformation registered in the Middle Pleistocene clays of site 2. (a) Main conjugate systems of extensional faults; (b) plot showing systems of fault planes and relative striae. (c) AMS ellipsoid measured for site SN05, showing the orientation of the maximum (square), intermediate (triangle) and minimum (circle) of the principal axes coherent with the direction of extension recognized through structural analysis.

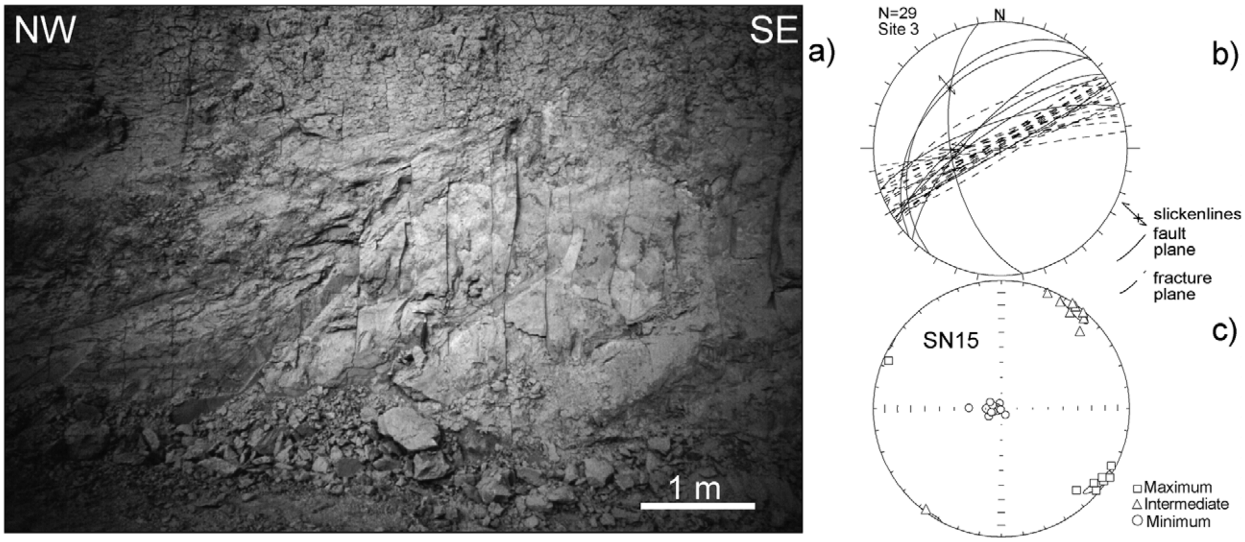

Fig. 10. Steeply-dipping ENE–WSW-trending fractures measured in site 3 ((a) and (b)) and maximum axis of the AMS ellipsoid oriented nearly perpendicular to these features (c).

magnetic lineations. Such a trend, which can be recognized both in Serravallian and Plio-Pleistocene sites, is confirmed by the structural data as it corresponds to the main extension direction derived from the fault population analysis on the NE–SW syn-sedimentary extensional fault system. A NW–SE extensional direction was already proposed by Catalano and Di Stefano (1997) for the Serravallian early syn-rift sedimentary sequences. The small number of sites that record an ENE–WSW- to E–W-directed magnetic lineation are associated with minor faults, which segment the main NE–SW extensional fault system with extensional to transtensional kinematics (Fig. 3). These fault strands, N–S- to NW–SE-trending, fit into the framework of the main NE–SW-oriented extensional fault system as transfer fault systems.

NW–SE-extension recorded by both the Serravallian and the Pliocene–Quaternary deposits attests that extensional processes in northeastern Sicily progressed during a continuous NW–SE extension direction. The Serravallian extensional basins recognized in northern Sicily are related

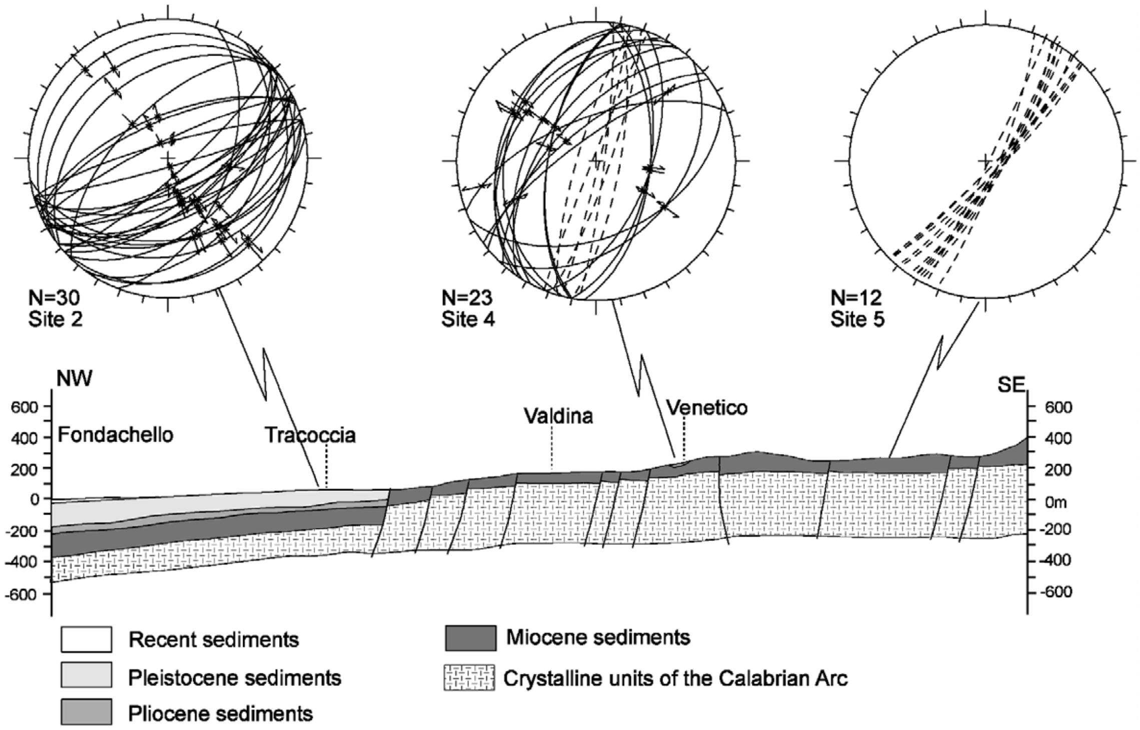

Fig. 11. Schematic profile crossing perpendicularly the main tectonic features recognized within the area (for the location see Fig. 3).

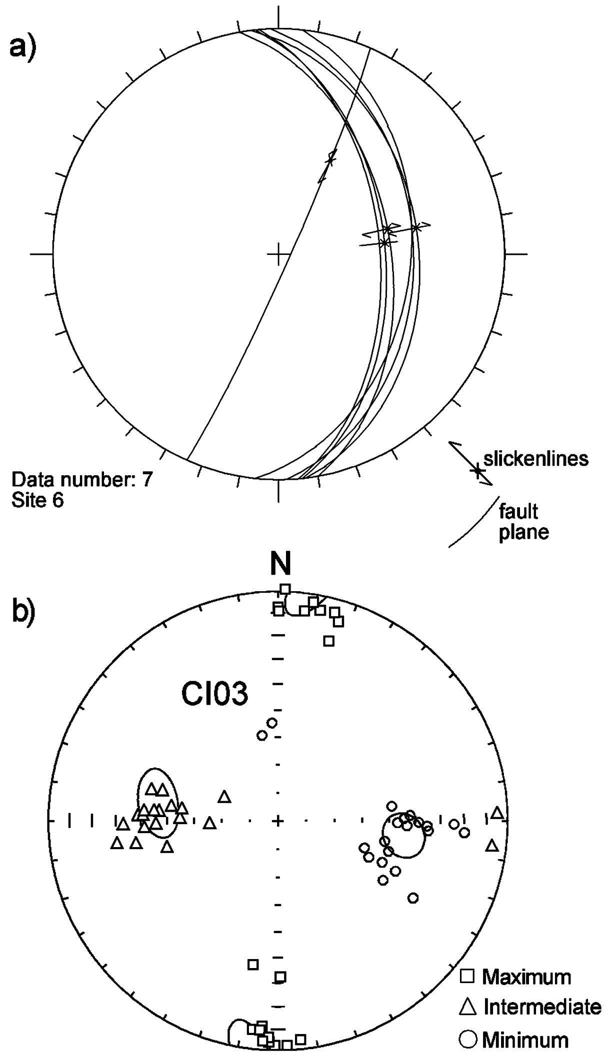

Fig. 12. (a) N–S-trending reverse faults measured in site 6 (Fig. 2). (b) The N–S oriented magnetic lineation for the paleomagnetic site CI03 (Fig. 2) suggests a mean E–W shortening direction, in agreement with the fault-slip analysis.

to the early stages of Tyrrhenian rifting, and represent the corresponding of the extensional basins that have been recognized both offshore of Sardinia (Sartori et al., 2001) and onshore in northern Calabria (Mattei et al., 2002).

Although the number of sites is limited, AMS and structural results from the foredeep domain investigated in the Catania basin indicate a compressional fabric, with magnetic lineation sub-parallel to the tilt axis. The N–S oriented magnetic lineation suggests a mean E–W shortening direction, which is in agreement with the fault-slip analyses carried out in the Misterbianco area by Labaume et al. (1990) and with our structural data in the eastern Catania foredeep at site 6 (Fig. 12). E–W shortening inferred from these data both in eastern and southern margins of Mt Etna is not compatible with a radial compression expected for the Etna volcano gravitational spreading, as suggested by Borgia et al. (1992, 2000). Conversely, our structural and AMS data support the idea of a regional scale compressive tectonics related to eastern transport of the Catania foredeep units. On the other hand, the E–W shortening direction is in contrast with the general south-eastward migration of the Gela nappe, recognized in southern Sicily (Butler et al., 1992). Based on the evidence that the present day geometry of the thrust front is not related to vertical axis rotations, we interpret this sector of the Gela nappe as a lateral ramp, whose geometry and orientation is controlled by the presence of the continental Hyblean foreland. A similar mechanism for the thrust emplacement has been proposed along the western border of the Gela nappe by Speranza et al. (1999).

It is worth noting that extensional tectonics is presently occurring along the eastern part of the Catania foredeep (Monaco and Tortorici, 2000), and that this tectonic deformation is not recorded in AMS fabric. These data confirm that AMS fabric in clay-rich units is mostly related to the early stages of deformation, and show that compressive tectonics in the eastern Catania foredeep occurred during lower-middle Pleistocene times (Di Stefano and Branca, 2002).

AMS results from the foreland domain in the Augusta area show a sub-horizontal magnetic foliation, sub-parallel to the bedding and an E–W-trending magnetic lineation. These data demonstrate that, in the Ionian foreland, the development of the sedimentary basins during Quaternary occurred and progressed under an E–W-trending extension, at least since the Middle Pleistocene. This provides a major constrain to the activity of the N–S-trending extensional system linked to the Malta escarpment in the onshore Hyblean Plateau. This also suggests that the NNW–SSE fault systems detected in the Ionian off-shore domain by Bianca et al. (1999), constitutes, during the Middle Pleistocene, the main tectonic feature of the study area, prevailing with respect to the NW–SE normal faulting related, in turn, to the northward sinking of the Hyblean foreland structure (Bianca et al., 1999; Adam et al., 2000; Monaco and Tortorici, 2000).

A large number of paleomagnetic data were previously collected in Mesozoic to Neogene sequences of the Sicilian Maghrebides chain, cropping out in central and western Sicily (Channell et al., 1980, 1990; Besse et al., 1984; Aifa et al., 1988; Scheepers et al., 1994; Duermeijer and Langereis, 1998; Speranza et al., 1999). A complex pattern of mainly clockwise rotations during the Neogene and the Quaternary have been determined, which contributed to the present day arcuate shape of the external front of the chain (Nairn et al., 1985; Channell et al., 1990; Scheepers and Langereis, 1994; Butler and Lickorish, 1997; Speranza et al., 2000). On the other hand, comparably fewer data have been collected in eastern Sicily. In the northern Tyrrhenian margin, clockwise rotations of about 20° have been measured in the Lower Pliocene of the Madonie Mts and in the Messina strait (Grasso et al., 1987; Aifa et al., 1988; Scheepers, 1994), whereas two sites collected in the Middle

Pleistocene sediments in the Milazzo region show no appreciable rotations (Scheepers, 1994). In the Hyblean foreland paleomagnetic data have been mainly collected in Mesozoic sequences (Grasso et al., 1983; Besse et al., 1984) and in few Early Pleistocene sites (Scheepers, 1994). All the data collected converge to show no significant rotations of the Hyblean foreland. Our paleomagnetic results demonstrate that no significant vertical axis rotations occurred in the Tyrrhenian back-arc, the Catania foredeep and the foreland basins (Fig. 13). The timing of the non-rotational tectonic regime can be constrained to the middle Pleistocene and, according to the result of site SN12 in the hinterland domain, could be extended back to the lower Pliocene. Counterclockwise rotations have been reported, however, in the Lower Pliocene Trubi Formation areas east of Villafranca and along the Messina Strait (Aifa et al., 1988; Scheepers et al., 1994). Our data concur with the results obtained by Scheepers and Langereis (1994) in middle Pleistocene units of the Milazzo area (Fig. 3), allowing extension of the no rotational regime in the hinterland domain back to Lower Pliocene.

Paleomagnetic results demonstrate that, independently from the different tectonic domains, non-rotational tectonic regimes are present in the whole region, at least since middle Pleistocene. This suggests that the progressive curvature of the Calabrian Arc and of the Sicilian nappes does not extend into the Middle Pleistocene. As a consequence, Pleistocene paleomagnetic rotations that have been measured in the Sicilian Maghrebides of western and central Sicily (Speranza et al., 1999) do not extend to the different tectonic domains of eastern Sicily. These rotations in western and central Sicily are most likely to local scale tectonic structures, which are related to the thrust and fold emplacement (Speranza et al., 2000).

9. Conclusions

AMS, paleomagnetic and structural data from eastern Sicily provide new constraints on the Quaternary tectonic evolution of the region. The magnetic lineation suggests that moving northward, the tectonic regime changed during the Quaternary, from E–W extension in the foreland domain, to E–W compression in the foredeep domain and NW–SE extension in the hinterland domain. The NW–SE extension orientation in northern Tyrrhenian margin is distinct from the E–W extensional direction in the eastern Hyblean plateau. The former is related to the extensional processes affecting the Tyrrhenian Sea, whereas the latter is mainly controlled by Quaternary activity of the Malta escarpment. Our results confirm that AMS is a valid tool for defining the deformation history in recent and undeformed sediments at the outcrop and regional scale. In conclusion, no paleomagnetic rotations have been found in the three tectonic domains of eastern Sicily since the Middle Pleistocene, and possible Lower Pliocene. These data allow us to define the upper limit to the curvature of the Calabrian Arc.

Acknowledgements

The Authors wish to thank M. Bianca and M. Porreca for field assistance. We also thank C. Faccenna for helpful discussion in the field. Processing of the structural data was performed through the software DAISY 2.2, kindly provided by F. Salvini. Funding is from the MURST 488/92 project (L. Tortorici). The paper benefited from the constructive reviews by Bernie Housen and Reinoud L.M. Vissers. ETH Contribution Nr. 1283.

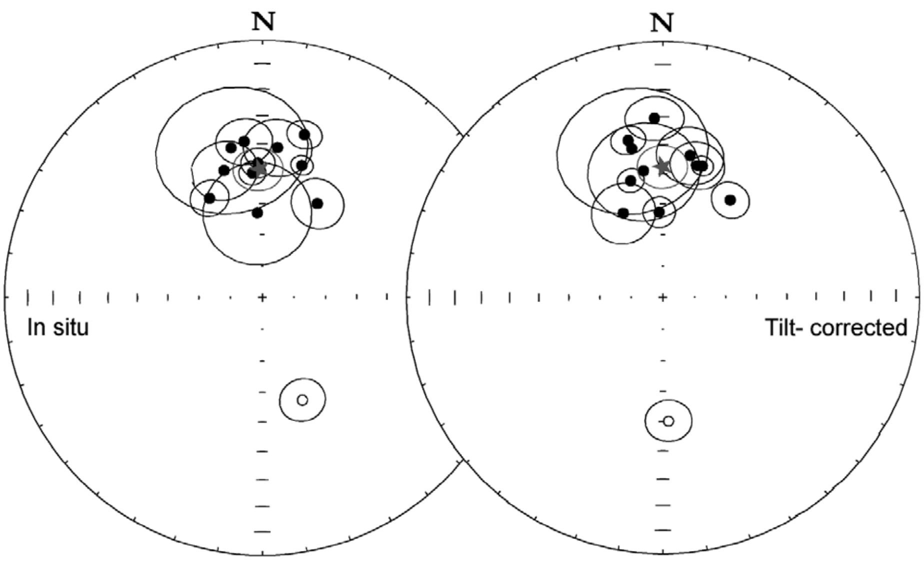

Fig. 13. Equal area projection of the site-mean direction from eastern Sicily. Open (solid) symbols represent projection onto upper (lower) hemisphere. Open ellipses are the projection of the α_{95} cones about the mean directions.

References

Adam, J., Reuther, C.D., Grasso, M., Torelli, L., 2000. Active fault kinematics and crustal stresses along the Ionian margin of southeastern Sicily. Tectonophysics 326, 217–239.

Aifa, T., Feinberg, H., Pozzi, J.P., 1988. Plio-Pleistocene evolution of the Tyrrhenizn arc: Paleomagnetic determination of uplift and rotational deformation. Earth and Planetary Science Letters 87, 438–452.

Aubourg, C., Rochette, P., Vialon, P., 1991. Subtle stretching lineation revealed by magnetic fabric of Callovian–Oxfordian black shales (French Alps). Tectonophysics 185, 211–223.

Besse, J., Pozzi, J.P., Mascle, G., Feinberg, H., 1984. Paleomagnetic study of Sicily: consequences for the deformation of Italian and African margins over the last 100 million years. Earth and Planetary Science Letters 67, 377–390.

Bianca, M., Monaco, C., Tortorici, L., Cernobori, L., 1999. Quaternary normal faulting in southern Sicily (Italy): a seismic source for the 1693 large earthquake. Geophysics Journal International 139, 370–394.

Bordonaro, S., Di Grande, A., Raimondo, W., 1984. Lineamenti geomorfostratigrafici pleistocenici tra Melilli, Augusta e Lentini (Siracusa). Bollettino Accademia Gioiena di Scienze Naturali, Catania 17, 65–88.

Bordoni, P., Valensise, G., 1998. Deformation of the 125-ka-marine terrace in Italy: tectonic implications. In: Stewart, I.S., Vita Finzi, C. (Eds.), Coastal Tectonics. Geological Society, Special Publication, 146, pp. 71–110.

Borgia, A., Ferrari, L., Pasquarè, G., 1992. Importance of gravitational spreading in the tectonic and volcanic evolution of Mount Etna. Nature 357, 231–235.

Borgia, A., Lanari, R., Sansosti, E., Tesauro, M., Bernardino, P., Fornaro, G., Neri, M., Murray, G.B., 2000. Actively growing anticlines beneath Catania from distal motion of Mount Etna's decollement measured by SAR interferometry and GPS. Geophysica Research Letters 27, 3409–3412.

Borradaile, G.J., 1988. Magnetic fabrics, petrofabrics and strain. Tectonophysics 156, 1–20.

Bosi, C., Carobene, L., Sposato, A., 1996. IL ruolo dell'eustatismo nella evoluzione geologica nell'area mediterranea. Memorie della Società Geologica Italiana 51, 363–382.

Butler, R.W.H., Lickorish, W.H., 1997. Using high resolution stratigraphy to date fold and thrust activity: examples from the Neogene of south-central Sicily. Journal of Geological Society of London 154, 633–643.

Butler, R.W.H., Grasso, M., La Manna, F., 1992. Origin and deformation of the Neogene-Recent Maghrebian foredeep at the Gela Nappe, SE Sicily. Journal of Geological Society of London 149, 547–556.

Catalano, R., D'Argenio, B., Montanari, L., Morlotti, E., Torelli, L., 1985. Marine geology of the Northwest Sicily offshore and its relationships with mainland structures. Bollettino della Società Geologica Italiana 104, 207–215.

Catalano, R., Di Stefano, P., Sulli, A., Vitale, F.P., 1996. Paleogeography and structure of the central Mediterranean: Sicily and its offshore area. Tectonophysics 260, 191–323.

Catalano, R., Doglioni, C., Merlini, S., 2001. On the Mesozoic Ionian Basin. Geophysical Journal International 144, 49–64.

Catalano, S., Di Stefano, A., 1997. Sollevamenti e tettogenesi pleistocenica lungo il margine tirrenico dei Monti Peloritani: integrazione dei dati geomorfologici, strutturali e biostratigrafic. Il Quaternario 10 (2), 337–342.

Channell, J.E.T., Catalano, R., D'Argenio, B., 1980. Paleomagnetism and deformation of the Mesozoic continental margin in Sicily. Tectonophysics 61, 391–407.

Channell, J.E.T., Oldow, J.S., Catalano, R., D'Argenio, B., 1990. Paleomagnetically determined rotations in the western Sicilian fold and thrust belt. Tectonics 9 (4), 641–660.

Dewey, J.F., Helman, M.L., Turco, E., Hutton, D.H.W., Knott, S.D., 1989. Kinematics of the Western Mediterranean. In: Coward, M.P., Dietrich D., Park R.G. (Eds.), Alpine Tectonics, Geological Society of London Special Publication 45, pp. 265–283.

Di Grande, A., Raimondo, W., 1982. Linee di costa plio-pleistoceniche e schema litostratigrafico del Quaternario siracusano. Geologica Romana 21, 279–309.

Di Stefano, A., Branca, S., 2002. Long-term uplift rate of the Etna volcano basement (southern Italy) based on biochronological data from Pleistocene sediments. Terra Nova 14, 61–68.

Duermeijer, C.E., Langereis, C.G., 1998. Astronomical dating of a tectonic rotation on Sicily and consequences for the timing and extent of a middle Pliocenedeformation phase. Tectonophysics 298, 243–258.

Faccenna, C., Mattei, M., Funiciello, R., Jolivet, L., 1997. Styles of back-arc extension in the Central Mediterranean. Terra Nova 9, 126–130.

Fisher, R.A., 1953. Dispersion on a sphere. Proceedings Royal Society of London 217, 195–305.

Gardiner, W., Grasso, M., Sedgeley, D., 1995. Plio-Pleistocene fault movement as evidence for mega-block kinematics within the Hyblean–Malta Plateau, Central Mediterranean. Journal of Geodynamics 19 (1), 35–51.

Gillot, P.Y., Kieffer, G., Romano, R., 1994. Evolution of Mt. Etna volcano in the light of potasium–argon dating. Acta Vulcanologica 5, 81–87.

Graham, J.W., 1966. Significance of magnetic anisotropy in Appalachian sedimentary rocks. In: Steinhart, J.S., Smith, T.J. (Eds.), The Earth Beneath the Continents. American Geophysical Union Geophysics, Monography 10, pp. 627–648.

Grasso, M., Lentini, F., 1982. Sedimentary and tectonic evolution of the eastern Hyblean Plateau (southeast Sicily) during Late Cretaceous to Quaternary times. Palaeogeography Palaeoclimatology Paleoecology 39, 261–280.

Grasso, M., Lentini, F., Nairn, A.E.M., Vigliotti, L., 1983. A geological and paleomagnetic study of the Hyblean volcanic rocks, Sicily. Tectonophysics 98, 271–295.

Grasso, M., Manzoni, M., Quintili, A., 1987. Misure magnetiche sui trubi infrapliocenici della Sicilia orientale: possibili implicazioni stratigrafiche e strutturali. Memorie della Società Geologica Italiana 38, 459–474.

Grasso, M., Reuther, C.D., Tortorici, L., 1992. Neotectonic deformations in SE Sicily: the Ispica fault, evidence of Late Miocene–Pleistocene decoupled wrenching within the Central Mediterranean Regime. Journal of Geodynamics 16 (1/2), 135–146.

Hailwood, E., Sayre, W., 1979. Magnetic anisotropy and sediments transport directions in North Atlantic Early Cretaceous black shales and Eocene mudstones cored on DSDP Leg 48. In: Montardent, L., Roberts, D., et al. (Eds.), Initial Report Deep Sea Drilling Project, 48. Washington, pp. 305–339.

Hamilton, N., Rees, A.I., 1970. The use of magnetic fabric in paleocurrent estimation. In: Runcorn, Sperling and Kupfer (Ed.), Peleogeophysics. Oxford, pp. 445–463.

Hirn, A., Nicolich, R., Gallart, J., Laigle, M., Cernobori, L., ETNASEIS Scientific Group, 1997. Roots of Etna volcano in faults of great earthquakes. Earth and Planetary Science Letters 148, 171–191.

Horvàth, F., 1993. Towards a mechanical model for the formation of the Pannonian basin. Tectonophysics 226, 333–357.

Housen, B.A., Richter, C., van der Pluijm, B.A., 1993. Composite magnetic anisotropy fabrics: experiments, numerical models, and implications for the quantification of rock fabrics. Tectonophysics 220, 1–12.

Hrouda, F., 1982. Magnetic anisotropy of rocks and its application in geology and geophysics. Geophysical Survey 5, 37–82.

Isacks, B., Molnar, P., 1971. Distribution of stresses in the descending lithosphere from a global survey of focal-mechanism solutions of mantle earthquakes. Review of Geophysics and Space Physics 9, 103–174.

Jelinek, V., 1977. The Statistical Theory of Measuring Anisotropy of Magnetic Susceptibility of Rocks and its Application, Geofyzika, Brno.

Jelinek, V., 1978. Statistical processing of anisotropy of magnetic susceptibility measured on groups of specimens and its applications. Studies Geophysical Geodesy 22, 50–62.

Jelinek, V., 1981. Characterisation of the magnetic fabrics of rocks. Tectonophysics 79, 63–67.

Kirschvink, J.L., 1980. The least-square line and plane and the analysis of paleomagnetic data. Geophysical Journal of Royal Astronomical Society 62, 699–718.

Kissel, C., Barrier, E., Laj, C., Lee, T.Q., 1986. Magnetic fabric in ≪undeformed≫ marine clays from compressional zones. Tectonics 5, 769–781.

Kissel, C., Laj, C., Lehman, B., Labyrie, L., Bout-Roumazeilles, V., 1997. Changes in the strength of the Iceland–Scotland Overflow Water in the last 200,000 years: evidence from magnetic anisotropy analysis of core SU90-33. Earth and Planetary Science Letters 152, 25–36.

Labaume, P., Bousquet, J.P., Lanzafame, G., 1990. Early deformations at submarine compressive front: the Quaternary Catania foredeep south of Mt. Etna, Sicily, Italy. Tectonophysics 177, 349–366.

Lee, T., Kissel, C., Laj, C., Horng, C.S., Lue, Y.T., 1990. Magnetic fabric analysis of the Plio-Pleistocene sedimentary formations of the Coastal Range of Taiwan. Earth and Planetary Science Letters 98, 23–32.

Lentini, F., Carbone, S., Catalano, S., Di Stefano, A., Gargano, C., Romeo, M., Strazzulla, S., Vinci, G., 1995. Sedimentary evolution of basins in mobile belts: examples from Tertiary terrigenous sequences of the Peloritani Mts (NE Sicily). Terra Nova 7, 161–170.

Lentini, F., Carbone, S., Catalano, S., Grasso, M., 1996. Elementi per la ricostruzione strutturale della Sicilia Orientale. Memorie della Società Geologica Italiana 51, 179–195.

Lentini, F., Catalano, S., Carbone, S., 2000. Carta geologica della Provincia di Messina, S.EL.CA. (Eds.), scale 1:50,000.

Lowrie, W., 1990. Identification of ferromagnetic minerals in a rock by coercivity and unblocking temperature properties. Geophysical Research Letters 17 (2), 159–162.

Lowrie, W., Hirt, A.M., 1987. Anisotropy of magnetic susceptibility in the Scaglia Rossa pelagic limestone. Earth and Planetary Science Letters 82, 349–356.

Lucente, F.P., Chiarabba, C., Cimini, G.B., Giardini, D., 1999. Tomographic constraints on the geodynamic evolution of the Italian region. Journal of Geophysical Research 104, 20307–20327.

Malinverno, A., Ryan, W.B.F., 1986. Extension in Tyrrhenian sea and shortening in the Apennines as result of arc migration driven by sinking of the lithosphere. Tectonics 5 (2), 227–254.

Mattei, M., Sagnotti, L., Faccenna, C., Funiciello, R., 1997. Magnetic fabric of weakly deformed clayey sediments in the Italian peninsula: relationships with compressional and extensional tectonics. Tectonophysics 271, 107–122.

Mattei, M., Speranza, F., Argentieri, A., Rossetti, F., Sagnotti, L., Funiciello, R., 1999. Extensional tectonics in the Amantea basin (Calabria, Italy): a comparison between structural and magnetic anisotropy data. Tectonophysics 307, 33–49.

Mattei, M., Cipollari, P., Cosentino, D., Argentieri, A., Rossetti, F., Speranza, F., Di Bella, L., 2002. The Miocene tectono-sedimentary evolution of the southern Tyrrhenian Sea: stratigraphy, structural and palaeomagnetic data from the on-shore Amantea basin (Calabrian Arc, Italy). Basin Research 14, 147–168.

McFadden, P.L., 1990. A new fold test for paleomagnetic studies. Geophysical Journal International 103, 163–169.

McFadden, P.L., McElhinny, M.W., 1988. The combined analysis of remagnetisation circles and direct observations in paleomagnetism. Earth and Planetary Science Letters 87, 161–172.

Monaco, C., 1997. Tettonica pleistocenica nell'area a sud dell'Etna (Sicilia orientale). Il Quaternario 10 (2), 393–398.

Monaco, C., Tortorici, L., 2000. Active faulting in the Calabrian arc and Eastern Sicily. Journal of Geodynamics 29, 407–424.

Monaco, C., Tapponier, P., Tortorici, L., Gillot, P.Y., 1997. Late Quaternary slip rates on the Acireale–Piedimonte normal faults and tectonic origin of Mt. Etna (Sicily). Earth and Planetary Science Letters 147, 125–139.

Nairn, A.E.M., Nardi, G., Gregor, C.B., Incoronato, A., 1985. Coherence of the Trapanese units during tectonic emplacement in western Sicily. Bollettino della Società Geologica Italiana 104, 267–272.

Nicolich, R., Laigle, M., Hirn, A., Cernobori, L., Gallart, J., 2000. Crustal structure of the Ionian margin of Sicily: Etna volcano in the frame of regional evolution. Tectonophysics 329, 121–139.

Ouliac, M., 1976. Removal of secondary magnetisation from natural remanent magnetization of sedimentary rocks: alternating field or thermal demagnetization technique? Earth and Planetary Science Letters 29, 65–70.

Pares, J.M., van der Pluijm, B.A., 2002. Evaluating magnetic lineations (AMS) in deformed rocks. Tectonophysics 350, 283–298.

Paterson, S.C., Yu, H., Oertel, G., 1995. Primary and tectonic fabric intensities in mudrocks. Tectonophysics 247, 105–119.

Pepe, F., Bertotti, G., Cella, F., Marsella, E., 2000. Rifted margin formation in the south Tyrrhenian Sea: high resolution seismic profile across the north Sicily passive continental margin. Tectonics 19 (2), 241–257.

Price, N.J., Cosgrove, J.W., 1990. Analysis of Geological Structures, Cambridge University Press, Cambridge.

Rees, A.I., 1965. The use of anisotropy of magnetic susceptibility in the estimation of sedimentary fabric. Sedimentology 4, 257–271.

Roberts, A.P., 1995. Magnetic properties of sedimentary greigite (Fe_3S_4). Earth Planetary Science Letters 134, 227–236.

Rochette, P., Jackson, M.J., Aubourg, C., 1992. Rock magnetism and the interpretation of anisotropy of magnetic susceptibility. Review of Geophysics 30 (3), 209–226.

Romano, R., 1982. Succession of the volcanic activity in the Etnean area. Memorie della Società Geologica Italiana 23, 27–38.

Sagnotti, L., Speranza, F., 1993. Magnetic fabric analysis of the Plio-Pleiatocene clay units of Sant'Arcangelo basin, southern Italy. Physics and Earth Planetary Interior 77, 165–176.

Sagnotti, L., Winkler, A., 1999. Rock magnetism and paleomagnetism of greigite-bearing mudstones in the Italian peninsula. Earth and Planetary Science Letters 165, 67–80.

Sagnotti, L., Faccenna, C., Funiciello, R., Mattei, M., 1994. Magnetic fabric and structural setting of Plio-Pleistocene clayey units in an extensional regime: the Tyrrhenian margin of central Italy. Journal of Structural Geology 16, 1243–1257.

Sagnotti, L., Speranza, F., Winkler, A., Mattei, M., Funiciello, R., 1998. Magnetic fabric of clay sediments from the external northern Apennines (Italy). Physics of the Earth and Planetary Interiors 105, 73–93.

Sartori, R., Carrara, G., Torelli, L., Zitellini, N., 2001. Neogene evolution of the southwestern Tyrrhenian Sea (Sardinia basin and western bathyal plain). Marine Geology 175, 47–66.

Scheepers, P.J.J., 1994. Tectonic rotations in the Tyrrhenian Arc system during the Quaternary and the Late Tertiary. Ph.D. thesis, University of Utrecht.

Scheepers, P.J.J., Langereis, C.G., 1994. Magnetic fabric of the Pleistocene clays from the Tyrrhenian arc: a magnetic lineation induced in the final stage of the middle Pleistocene compressive event. Tectonics 13, 1190–1200.

Scheepers, P.J.J., Langereis, C.G., Zijderveld, J.D.A., Hilgen, F.G., 1994. Paleomagnetic evidence for a Pleistocene clockwise rotation of the Calabro-Peloritan block (southern Italy). Tectonophysics 230, 19–48.

Schieber, J., Ellwood, B.B., 1988. Determination of basinwide paleocurrent patterns in a shale succession from anisotropy of magnetic susceptibility (AMS): a case study of the Mid-Proterozoic Newland Formation, Montana. Journal of Sedimentary Petrology 58, 830–835.

Speranza, F., Maniscalco, R., Mattei, M., Di Stefano, A., Butler, R.W.H., Funiciello, R., 1999. Timing and magnitude of rotation in the frontal thrust system of southwestern Sicily. Tectonics 18 (6), 1178–1197.

Speranza, F., Maniscalco, R., Mattei, M., Funiciello, R., 2000. Paleomagnetism in the Sicilian Maghrebides: review of the data and implications for the tectonic styles and shortening estimates. Memorie della Società Geologica Italiana 55, 95–102.

Tarling, D.H., Hrouda, F., 1993. The Magnetic Anisotropy of Rocks, Chapman and Hall, London.

Torelli, L., Grasso, M., Mazzoldi, G., Peis, D., 1998. Plio-Quaternary tectonic evolution and structure of the Catania foredeep, the northern Hyblean Plateau and the Ionian shelf (SE Sicily). Tectonophysics 298, 209–221.

Tortorici, L., Monaco, C., Tansi, C., Cocina, O., 1995. Recent and active tectonics in the Calabrian Arc (Southern Italy). Tectonophysics 243, 37–55.

Wernicke, B., Burchfield, B.C., 1982. Modes of extensional tectonics. Journal of Structural Geology 4, 105–115.

Wezel, F.C., 1967. I terreni quaternari del substrato dell'Etna. Atti Accademia Gioiena Scienze Naturali Catania 6 (XVIII), 271–282.